Development 133, 351-361 doi:10.1242/dev.02204

Retinaldehyde dehydrogenase 2 (RALDH2)-mediated retinoic acid synthesis regulates early mouse embryonic forebrain development by controlling FGF and sonic hedgehog signaling

Vanessa Ribes[1,*], Zengxin Wang[2,*], Pascal Dollé[1,†] and Karen Niederreither[2,†]

Although retinoic acid (RA) has been implicated as one of the diffusible signals regulating forebrain development, patterning of the forebrain has not been analyzed in detail in knockout mouse mutants deficient in embryonic RA synthesis. We show that the retinaldehyde dehydrogenase 2 (RALDH2) enzyme is responsible for RA synthesis in the mouse craniofacial region and forebrain between the 8- and 15-somite stages. *Raldh2*$^{-/-}$ knockout embryos exhibit defective morphogenesis of various forebrain derivatives, including the ventral diencephalon, the optic and telencephalic vesicles. These defects are preceded by regionally decreased cell proliferation in the neuroepithelium, correlating with abnormally low D-cyclin gene expression. Increases in cell death also contribute to the morphological deficiencies at later stages. Molecular analyses reveal abnormally low levels of FGF signaling in the craniofacial region, and impaired sonic hedgehog signaling in the ventral diencephalon. Expression levels of several regulators of diencephalic, telencephalic and optic development therefore cannot be maintained. These results unveil crucial roles of RA during early mouse forebrain development, which may involve the regulation of the expansion of neural progenitor cells through a crosstalk with FGF and sonic hedgehog signaling pathways.

KEY WORDS: Retinoids, Forebrain development, Eye development, Neural crest, Telencephalon, Diencephalon, Optic vesicle, Pituitary, Sonic hedgehog, FGF, Mouse, *Aldh1a2*

INTRODUCTION

The embryonic forebrain is the most anterior neural plate derivative that will give rise to brain centers controlling perceptions, memory, emotions, voluntary movements and endocrine functions. Its morphogenesis relies on multiple interactions with non-neural tissues, including the prechordal axial mesendoderm, the head mesoderm and, later on, the lens and olfactory placodes (Gong and Shipley, 1995; Pera and Kessel, 1997; Graham and Begbie, 2000). At the end of anterior neuropore closure, the forebrain is subdivided into the anteriorly positioned telencephalon and eye field, and the more caudal diencephalon, which will contribute to the prethalamus, thalamus and pretectum, and ventrally to the hypothalamus (reviewed by Puelles and Rubenstein, 2003; Wilson and Houart, 2004). At this stage, neural progenitors have acquired their spatial identity, defined by distinct combinations of transcription factors (Shimamura et al., 1997; Chow and Lang, 2001; Crossley et al., 2001; Kobayashi et al., 2002). Several secreted molecules, including sonic hedgehog (SHH), fibroblast growth factors (FGFs), WNTs and bone morphogenetic proteins (BMPs), as well as retinoic acid (RA), have been implicated in early forebrain regionalization (reviewed by Rallu et al., 2002a; Echevarria et al., 2003; Wilson and Houart, 2004).

RA is a diffusible lipophilic molecule that binds to nuclear receptors, the RARs (α, β and γ), which act as RXR heterodimers to regulate the transcription of target genes (reviewed by Chambon, 1996). In mice, the three RARs are expressed in different embryonic head tissues (Ruberte et al., 1991; Mollard et al., 2000), and RARα-RARγ double mutants lack some frontonasal process derivatives and display brain abnormalities, especially of the telencephalic vesicles (Lohnes et al., 1994). Studies in avian models have revealed sequential roles for RA signaling during forebrain development. Analysis of RA-deficient quail embryos has implicated RA as an early signal acting during gastrulation to regulate anteroposterior (AP) patterning of the neural plate (Halilagic et al., 2003). Later on, RA is required for the survival of anterior head mesenchymal cells and the development of telencephalic structures (Schneider et al., 2001; Halilagic et al., 2003). RA has also been implicated as a signal specifying an intermediate character within the telencephalon (Marklund et al., 2004). These studies have highlighted possible crossregulatory interactions between RA and two signals emanating from local forebrain organizers: FGF signaling from the anterior neural ridge (ANR) (Shimamura and Rubenstein, 1997; Ohkubo et al., 2002); and SHH signaling from the prechordal plate and ventral diencephalon (Ericson et al., 1995; Gunhaga et al., 2000).

The tissue distribution and levels of RA are controlled by the activities of synthesizing enzymes, the retinaldehyde dehydrogenases (RALDHs), and of metabolizing enzymes, the cytochrome P450s CYP26 (reviewed by Duester, 2001; Stoilov et al., 2001). The *Raldh2* (*Aldh1a2* – Mouse Genome Informatics) and *Raldh3* (*Aldh1a3* – Mouse Genome Informatics) genes are differentially activated during early embryonic head and forebrain development. *Raldh2* is transiently expressed in the anteroventral neuroepithelium prior to optic vesicle outgrowth (Wagner et al., 2000; Smith et al., 2001), whereas *Raldh3* is expressed later, although more persistently, in the surface ectoderm overlying the anterior forebrain neuroepithelium and optic vesicle (Li et al., 2000; Schneider et al., 2001; Blentic et al., 2003). Although RALDH3 is often mentioned as the principal RA-synthesizing acting during

[1]Institut de Génétique et de Biologie Moléculaire et Cellulaire, CNRS, INSERM, Université Louis Pasteur, BP 10142, 67404 Illkirch Cedex, CU de Strasbourg, France. [2]Departments of Medicine and Molecular and Cellular Biology, Baylor College of Medicine, One Baylor Plaza, Houston, Texas 77030, USA.

*These authors contributed equally to this work
†Authors for correspondence (e-mail: karenn@bcm.tmc.edu; dolle@igbmc.u-strasbg.fr)

Accepted 9 November 2005

patterning of the forebrain (Schneider et al., 2001; Marklund et al., 2004), no developmental or molecular forebrain abnormalities have been reported in *Raldh3*$^{-/-}$ knockout mice, which die at birth because of nasal defects (Dupé et al., 2003). However, *Raldh2*$^{-/-}$ mutants, which die between embryonic days (E) 9.5 and 10.5 owing to defective heart development, exhibit an externally truncated forebrain and frontonasal region (Niederreither et al., 1999), as well as impaired optic vesicle morphogenesis (Mic et al., 2004a).

We have studied the cellular and molecular defects underlying abnormal forebrain development in these mutants. Using a RA-sensitive reporter transgene, we show that RALDH2 is responsible for all detectable RA activity in the mouse forebrain and craniofacial tissues until the 14- to 15-somite-stages. Lack of RA synthesis, at these stages, drastically affects forebrain morphogenesis. By perturbing efficient FGF and SHH signaling, RA deficiency alters cell proliferation and survival, as well as expression levels of important regulators of ventral forebrain development.

MATERIALS AND METHODS

Raldh2-null mutant mice have been described previously (Niederreither et al., 1999). Whole-mount in situ hybridization with digoxigenin-labeled riboprobes was performed as described (Chotteau-Lelièvre et al., 2005), using Intavis InSituPro robots (for a detailed procedure, see http://www.eumorphia.org/EMPReSS/servlet/EMPReSS.Frameset, Gene Expression section). Whole-mount X-gal assays were performed as described (Rossant et al., 1991). Whole-mount immunolabeling with the phospho-p44/p42 Map-kinase (p-ERK1/2) antibody (Cell Signaling) was performed according to the Rossant laboratory protocol (http://www.mshri.on.ca/rossant/protocols/DpERK%20Immunohistochem.html). Immunolabeling with rabbit polyclonal anti-PAX6 (Babco) and anti-RALDH2 (Berggren et al., 1999) was performed as described (Scardigli et al., 2003), using a peroxidase-conjugated goat anti-rabbit (Jackson Immunoresearch) secondary antibody. Immunohistochemistry with anti-phospho-Histone H3 (Upstate) were performed on 10 μm cryosections. Procedures for conventional histology and TUNEL assays can be found at http://www.eumorphia.org/EMPReSS/servlet/EMPReSS.Frameset (Necropsy exam, Pathology and Histology section). Three to eight *Raldh2*$^{-/-}$ embryos were examined for all assays and at each developmental stage described hereafter.

RESULTS

RALDH2 is responsible for RA signaling in the early embryonic head

To assess RALDH2 function during head development, we first analyzed its protein expression in wild-type mouse embryos. RALDH2 protein was first detected by the seven- to eight-somite-stages (E8.0) (data not shown) and was strongly expressed within the anterior forebrain neuroepithelium, including most of the optic evagination and presumptive telencephalon, at the 10- to 12-somite stages (Fig. 1A,A′). Weaker signal was seen in the overlying surface ectoderm (Fig. 1A′). By the 14- to 15-somite stages, RALDH2 expression had mostly receded from the forebrain neuroepithelium (Fig. 1E,E′), whereas surface ectoderm expression remained strong until E9.5 (Fig. 1I,I′). Some RALDH2-positive cells were also detected in the mesenchyme caudally to the optic vesicles (Fig. 1I′). Immunostaining of *Raldh2*$^{-/-}$ knockout embryos showed no signal, excluding a crossreactivity with RALDH3 (Fig. 1I, inset).

To assess the contribution of RALDH2 in mediating active RA signaling in the embryonic head, we analyzed the activity of the *RARE-hsp68-lacZ* transgene (Rossant et al., 1991), a sensitive reporter for endogenous RA signaling (e.g. Wagner et al., 2000; Niederreither et al., 2002a; Mic et al., 2004b), in wild-type and *Raldh2*$^{-/-}$ embryos. In eight- to 12-somite stage wild-type embryos, the transgene was expressed in a region of the forebrain encompassing the optic vesicles (Fig. 1B,B′) and eventually the outgrowing telencephalon (Fig. 1F,F′,J,J′), but excluding the ANR and the diencephalon (Fig. 1B′,F′,J′). The RA-reporter transgene was also activated between the 10- and 14-somite stages in the anterior head mesenchyme and surface ectoderm (Fig. 1B′,F′,J′). In *Raldh2*$^{-/-}$ embryos, no transgene activity was detected prior to the 14- to 15-somite stages, when expression first appeared in scattered ectodermal cells in the optic region (Fig. 1C,G). *Raldh3* gene expression was induced at a slightly earlier stage (10-12 somites) in both wild-type and *Raldh2*$^{-/-}$ embryos (Fig. 1D), and was then expressed at comparable levels in the head ectoderm of wild-type and mutants (Fig. 1H,L). Thus, the altered induction of the RA-reporter transgene in *Raldh2*$^{-/-}$ embryos cannot be attributed to a

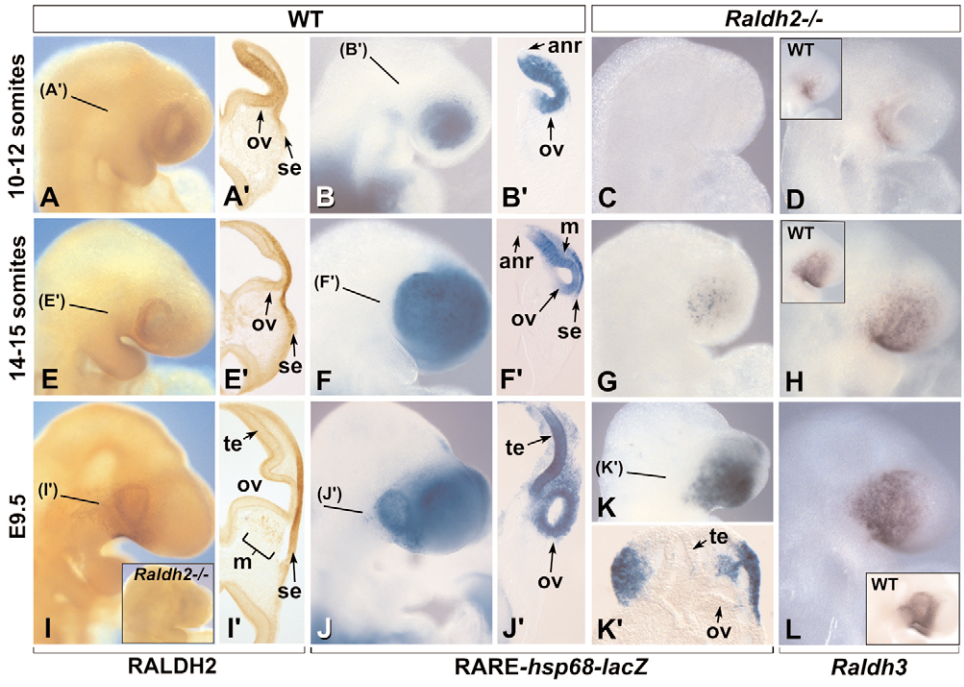

Fig. 1. RALDH2 mediates RA signaling at early stages of embryonic craniofacial development. (**A**-**L**) RALDH2 protein distribution (A,E,I), β-galactosidase activity of the *RARE-hsp68-lacZ* transgene (B,C,F,G,J,K) and *Raldh3* mRNA (D,H,L) were analyzed at successive stages (as indicated on the left) in wild-type and *Raldh2*$^{-/-}$ embryos (as indicated above). (A′-K′) Transverse sections at levels indicated (black lines) in the main panels. Insets show stage-matched embryos of the alternate genotype. anr, anterior neural ridge; m, mesenchyme; ov, optic vesicle; se, surface ectoderm; te, telencephalon.

downregulation of *Raldh3* gene expression. At later stages, transgene activity expanded in the facial region of *Raldh2*$^{-/-}$ embryos (Fig. 1K). Section analysis showed activity in both the surface ectoderm and underlying mesenchyme (Fig. 1K′); however, the forebrain and optic vesicle neuroepithelium were almost completely devoid of transgene activity (compare Fig. 1J′ with 1K′).

Together, these data show that RALDH2 activity accounts for the region-specific patterns of RA-response observed in the early forebrain neuroepithelium and the adjacent mesenchyme. Upon RALDH2 deficiency, RALDH3 activity cannot significantly induce the RA-reporter transgene within the forebrain neuroepithelium, although it can eventually activate it in surface ectoderm and mesenchyme, with a delay of about half a day when compared with wild-type embryos.

Raldh2 deficient embryos display defective forebrain and optic development

Raldh2$^{-/-}$ knockout embryos have an externally truncated craniofacial region (Niederreither et al., 1999). Detailed histological analysis was performed to characterize the underlying defects. No abnormality was observed in mutants at presomitic stages (data not shown). At the 10- to 12-somite stages, before anterior neuropore closure, the optic sulci did not evaginate properly in *Raldh2*$^{-/-}$ embryos (Fig. 2A-B′) and the cellular architecture of the forebrain neuroepithelium was regionally disorganized (Fig. 2B,B′, brackets). At the 15- to 16-somite stages, the neuroepithelium was disorganized and misfolded along the optic vesicle-diencephalic junction (Fig. 2C,D), and cell debris were seen in the ventricular lumen (Fig. 2D, arrowheads). No evagination of the prospective telencephalic vesicles was seen in mutant embryos (Fig. 2E,F). Throughout these stages, an abnormal accumulation of loose mesenchymal cells was observed in the frontonasal region of *Raldh2*$^{-/-}$ embryos (Fig. 2B′,F).

By E9.5, telencephalic and diencephalic vesicles have formed in wild-type embryos (Fig. 2G). *Raldh2*$^{-/-}$ embryos displayed a single, hypoplastic forebrain vesicle with no visible constriction between telencephalic and diencephalic territories (Fig. 2H). All forebrain structures, i.e. the telencephalon, optic vesicles, diencephalon and hypothalamus, were hypoplastic (Fig. 2I,J); the corresponding neuroepithelium appeared abnormally thin (Fig. 2G-J; adjacent mesencephalic neuroepithelium are of normal thickness, see insets in G,H).

Eye development was compromised in *Raldh2*$^{-/-}$ mutants, whose optic vesicles did not closely contact the surface ectoderm (Fig. 2I,J, insets), an event that is indispensable for lens placode induction and optic pit formation. The development of Rathke's pouch was also affected. This structure appears by invagination of an ectodermal placode in the stomodeum (primitive mouth cavity), that will contact the forebrain floor plate (infundibulum) to form the pituitary anlage (Fig. 2K). Rathke's pouch was absent in most of the *Raldh2*$^{-/-}$ embryos (Fig. 2L; *n*=9/12). A thin cord of cells was seen ventrally to the infundibulum, which was molecularly identified as a prechordal plate remnant (Fig. 2L; see Fig. 8D). In some mutants (*n*=3/12), a rudimentary pouch was present (Fig. 2M). *Raldh2*$^{-/-}$ embryos were not analyzed after E9.5, as they die about 1 day later because of cardiovascular defects (Niederreither et al., 2001).

Abnormal patterns of cell death and cell proliferation contribute to the *Raldh2*$^{-/-}$ forebrain defects

TUNEL analysis was performed to assess whether abnormal apoptosis may contribute to the forebrain abnormalities in *Raldh2*$^{-/-}$ mutants. No abnormal cell death was detected in mutants prior to the 14-somite stage (data not shown). From this stage,

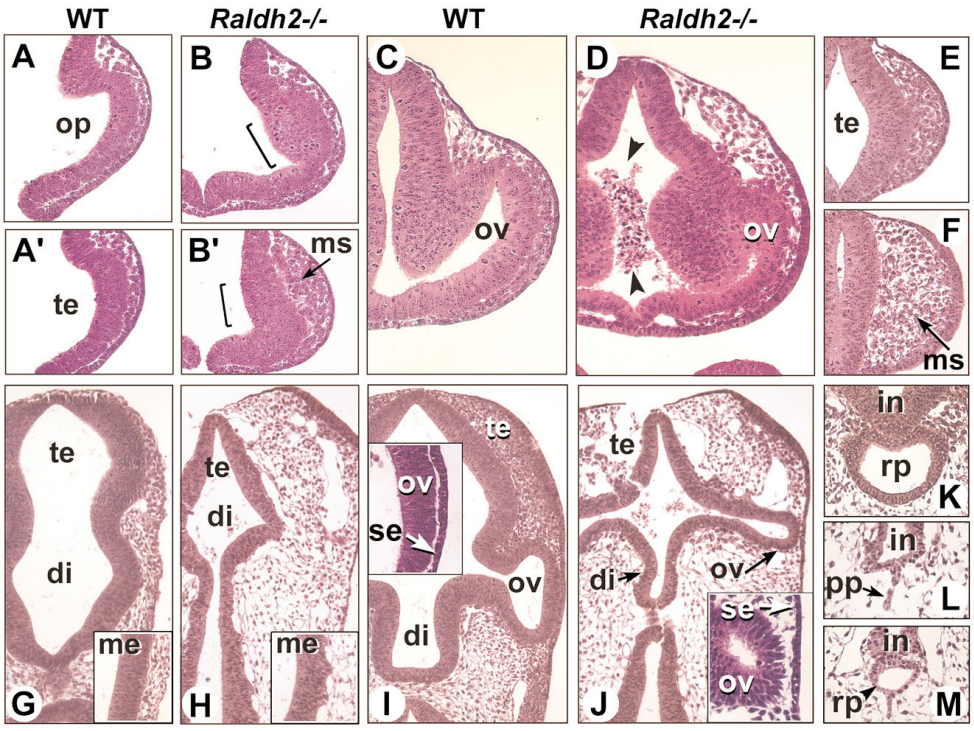

Fig. 2. Defective forebrain and optic development in *Raldh2*$^{-/-}$ embryos. (**A**,**A′**) Serial frontal sections through the forebrain neuroepithelium of a headfold (10 somite)-stage wild-type embryo at the level of the optic evagination (ov) and prospective telencephalon (te). (**B**,**B′**) Comparative sections of a stage-matched *Raldh2*$^{-/-}$ embryo. Brackets indicate regionally disorganized neuroepithelium. There is an excess of overlying mesenchymal cells (ms). (**C**,**D**) Comparative frontal sections at an early stage of optic vesicle (ov) development (14- to 15-somite stages). Arrowheads indicate the presence of cell debris in the *Raldh2*$^{-/-}$ forebrain lumen. (**E**,**F**) Sections at the anterior forebrain level, showing defective telencephalic vesicle outgrowth and excess mesenchymal cells (in the mutant, F). (**G**-**J**) Serial transverse sections through the telencephalic (te), diencephalic (di) and optic (ov) vesicles of E9.5 wild-type (G,I) and *Raldh2*$^{-/-}$ (H,J) embryos. Insets show details of the mesencephalic (me) neuroepithelium (G,H) and of the distal tip of the optic vesicle and surface ectoderm (se) (I,J). (**K**-**M**) Details of the infundibulum (in) and Rathke's pouch (rp) in a control (K) and two *Raldh2*$^{-/-}$ (L,M) embryos. pp, prechordal plate. Hematoxylin and Eosin staining.

abnormal apoptosis was detected in the optic vesicle and infundibulum neuroepithelium (Fig. 3A,B), in the area that was found to be disorganized upon histological analysis (Fig. 2D). Between E8.5 and E9.5, apoptosis extended within the forebrain neuroepithelium to reach the intermediate telencephalic region, and was also seen among pre-optic mesenchymal cells (data not shown). Furthermore, whole-mount TUNEL analysis showed an abnormal distribution of apoptotic cells in the rostral surface ectoderm of E9.5 mutants, contrasting with the restricted apoptosis along the ventral midline and placodal ectoderm of wild-type embryos (Fig. 3C,D).

To assess whether abnormal cell proliferation may account for the forebrain neuroepithelium hypoplasia in *Raldh2*$^{-/-}$ embryos, phosphorylated histone H3 immunodetection was performed on both whole mounts and sections. No significant difference in the numbers of mitotic cells was observed in the forebrain neuroepithelium or mesenchyme of *Raldh2*$^{-/-}$ versus wild-type embryos, up to the 12-somite stage (data not shown). From the 14-somite stage, cell proliferation was diminished in the mutant ventral forebrain neuroepithelium, especially along the diencephalon and optic vesicle (Fig. 3E-G). At E9.5, proliferation was almost abolished in the mutant forebrain, except in its dorsalmost region (data not shown). Interestingly, at this stage, expression of the cell cycle inhibitor *p21* (Sherr and Roberts, 1999) was detected in the ventral forebrain neuroepithelium of mutants (Fig. 3I), whereas in wild-type littermates it was only observed in the maxillary ectoderm (Fig. 3H). We also analyzed the expression of D-cyclin genes, components of the cell cycle machinery that are dynamically expressed during embryogenesis (Wianny et al., 1998). At the 14-somite stage, cyclin D1 expression in head mesenchymal cells was similar in *Raldh2*$^{-/-}$ and wild-type embryos (data not shown). However, cyclin D2 expression was reduced in the diencephalic neuroepithelium, and almost undetectable in the prospective telencephalon of mutant embryos, while expression at mesencephalic levels was comparable with wild-type embryos (Fig. 3J,K). Cyclin D3 expression was also downregulated in the forebrain neuroepithelium of *Raldh2*$^{-/-}$ embryos, except in the ventralmost telencephalon (Fig. 3L,M).

Abnormal craniofacial neural crest distribution

Neural crest cells (NCCs) that colonize the frontonasal and peri-optic regions originate from prosencephalic and mesencephalic levels (Serbedzija et al., 1992; Osumi-Yamashita et al., 1994). To investigate whether the excess mesenchyme observed in the frontonasal area of *Raldh2*$^{-/-}$ embryos (see Fig. 2) corresponds to NCCs, we used *Crabp1* and *AP2α* as markers of migrating NCCs. This analysis confirmed that mesenchymal cells in *Raldh2*$^{-/-}$ mutants mostly correspond to NCCs (Fig. 4A,B, insets). Furthermore, whole-mount analysis indicated a deficit of NCCs posteriorly to the optic vesicle (Fig. 4A,B, brackets), while numerous NCCs were found in the pre-optic mesenchyme of 13-14 somite-stage *Raldh2*$^{-/-}$ embryos (Fig. 4D, arrow). At E9.5, NCCs were mainly located along the rostroventral edge of the frontonasal process in wild-type embryos, whereas these were distributed throughout the frontonasal region in mutants (Fig. 4C,D, insets).

We also analyzed NCC molecular determinants that are induced before the lethality of *Raldh2*$^{-/-}$ embryos. *Sox9* is required for chondrogenic determination of cranial NCCs (Mori-Akiyama et al., 2003), whereas *Sox10* is thought to maintain the pluripotency of NCCs, and at later stages to direct a non-neuronal fate (Kim et al., 2003). Both of these determinants were induced in the cranial NCCs of *Raldh2*$^{-/-}$ embryos (Fig. 4E-H). The abnormal *Sox10* pattern, which was massively expressed within the frontonasal area (Fig. 4F, arrow), may reflect the abnormal distribution of NCCs and/or indicate that these cells are arrested at a multipotent state.

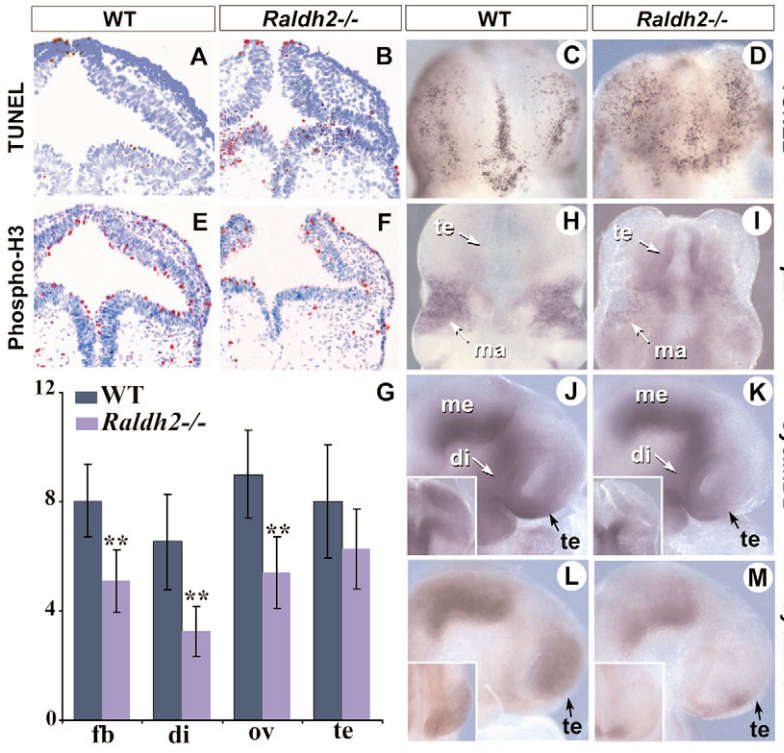

Fig. 3. Region-specific apoptosis and defective cell proliferation in the RA-deficient forebrain. (**A**,**B**) Immunofluorescent TUNEL detection of apoptotic cells on transverse forebrain sections of 14- to 15-somite stage wild-type (A) and *Raldh2*$^{-/-}$ (B) embryos. Overlays of the DAPI nuclear staining (blue) and TUNEL signal (red) are shown in false colors. (**C**,**D**) Whole-mount TUNEL analysis of wild type (C) and mutant (D) E9.5 embryos. Frontal views of the head. (**E**,**F**) Immunofluorescent detection of phospho-histone H3 on transverse forebrain sections of 14- to 15-somite stage embryos (false color overlays as in A,B). (**G**) Numbers of phospho-histone H3-positive cells as percentages of total cell numbers along the whole ventral forebrain neuroepithelium (fb) and three subregions, the rostroventral diencephalon (di), optic vesicles (ov) and ventral telencephalon (te) of 14-somite stage wild-type and *Raldh2*$^{-/-}$ embryos. Four embryos of each genotype were sectioned transversely, and all sections encompassing the aforementioned regions were counted (fb: wild type, 8%±1.3; mut, 5.1%±1.1; mean±s.e.m.; *t*-test P=0.0147; di: wild type, 6.5%±1.7; mut, 3.3%±0.9; P=0.0158; ov: wild type, 8.9%±1.6; mut, 5.4%±1.3; P=0.0131; te: wild type, 8.0%±2.0; mut, 6.3%±1.5; P=0.219). (**H**-**M**) Whole-mount in situ hybridization of *p21* (H), cyclin D2 (J,K) and cyclin D3 (L,M) in wild-type and *Raldh2*$^{-/-}$ embryos. H,I: ventral views of E9.5 heads; J-M: profile views of 13- to 14-somite stage embryos. Insets show ventral (J,K) and frontal (L,M) views of the forebrain. ma, maxillary process; me, mesencephalon.

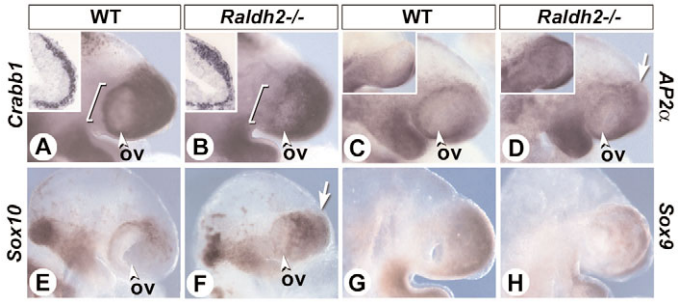

Fig. 4. Abnormal distribution of facial neural crest cells in *Raldh2*$^{-/-}$ embryos. Whole-mount in situ hybridization of *Crabp1* (**A**,**B**), *Ap2a* (**C**,**D**), *Sox10* (**E**,**F**) and *Sox9* (**G**,**H**). Profile views. Embryos are at 12-14 somites (A-F) or E9.5 (G,H, and insets in C,D). Genotypes are indicated above. Brackets (A,B) indicate a deficit of labeled cells in the post-optic area, and arrows (D,F) indicate an excess of labeled cells in the preoptic (frontonasal) region of mutant embryos. ov, optic vesicle. Insets in A,B show transverse sections of 13- to 14-somite stage embryos.

Maintenance of telencephalic gene expression requires *Raldh2* activity

We then investigated whether regionalization of the forebrain is affected in *Raldh2*$^{-/-}$ embryos. The winged helix transcription factor *Foxg1* (*Bf1*) is expressed in the telencephalic field from the five-somite stage (Shimamura et al., 1995) (Fig. 5A,C) and is required for the development of telencephalic structures (Xuan et al., 1995). *Foxg1* expression was normally induced in *Raldh2*$^{-/-}$ embryos until the 13-somite stage (data not shown), but became abnormally weak by the 15-somite stage (Fig. 5A,B), especially in the intermediate telencephalon. By E9.5, its expression was almost extinguished, with residual expression towards the ventral edge of the *Raldh2*$^{-/-}$ forebrain (Fig. 5C,D).

We analyzed another telencephalic determinant, *Emx2*, whose expression is restricted to dorsal forebrain territories (Simeone et al., 1992). *Emx2* was correctly induced in the telencephalon of 10-somite stage *Raldh2*$^{-/-}$ embryos (Fig. 5E,F). However, at E9.5, *Emx2* transcripts were expressed at relatively low and homogeneous levels along the neuroepithelium that failed to develop telencephalic vesicles, rather than according to a dorsal-to-ventral gradient as in wild-type embryos (Fig. 5G,H). Such a pattern was reminiscent of that observed in wild-type and mutant embryos at an earlier stage, before telencephalic vesicle outgrowth (Fig. 5E,F, insets).

We then analyzed how ventral cell fates are determined in the *Raldh2*$^{-/-}$ forebrain. The *Nkx2.1* homeobox gene is expressed in ventral regions of the prospective diencephalon and telencephalon (Fig. 5I) The *Nkx2.1* expression domain was reduced in *Raldh2*$^{-/-}$ embryos already at the 11-somite stage (Fig. 5I,J). Diencephalic expression was the most severely affected and *Nkx2.1* transcripts were detected, albeit at lower levels, in the ventral telencephalon of *Raldh2*$^{-/-}$ embryos (Fig. 5I,J, insets). *Nkx2.1* diencephalic expression remained markedly downregulated in mutants at E9.5, although the ventralmost diencephalic cells showed higher transcript levels (Fig. 5K,L). At this stage, *Nkx2.1* expression in the wild-type telencephalon demarcates the future medial ganglionic eminence (Fig. 5K). The corresponding *Nkx2.1*-positive domain was both spatially and quantitatively reduced in the mutant embryos (Fig. 5L).

We also assessed whether the onset of neuronal differentiation is affected in the RA-deficient forebrain by analyzing *Delta1* (Bettenhausen et al., 1995) and *Hes5* (Hatakeyama et al., 2004), which respectively encode a ligand and a downstream effector of the Notch pathway. Although the first *Delta1*-expressing cells were

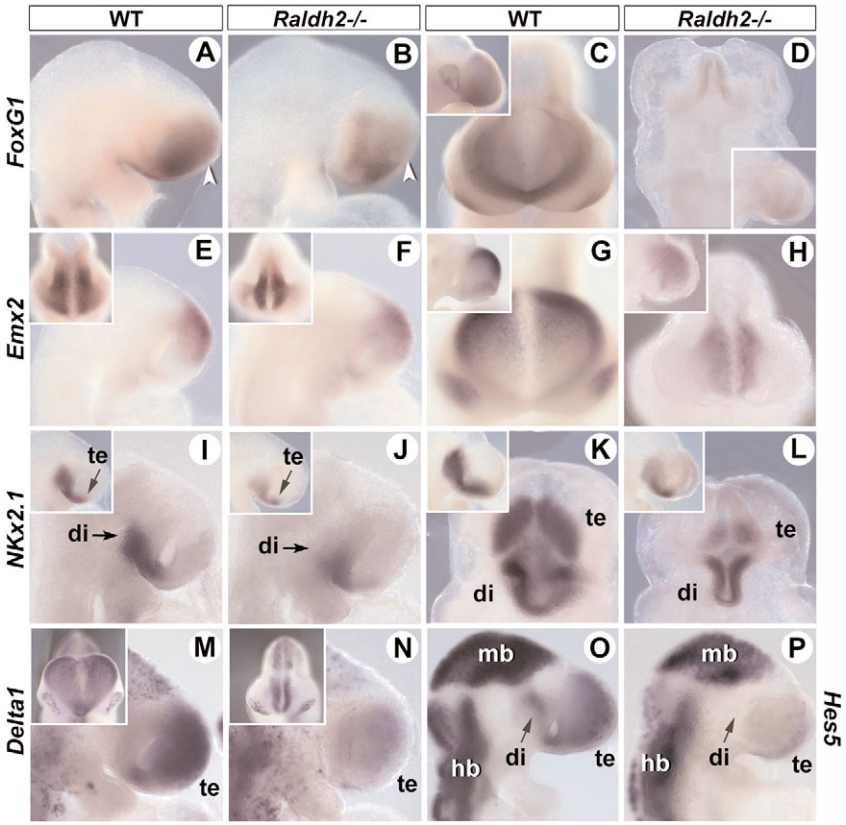

Fig. 5. Molecular analysis of forebrain development in *Raldh2*$^{-/-}$ embryos. Whole-mount in situ hybridization of *Foxg1* (**A**,**B**: 13-14 somites; **C**,**D**: E9.5), *Emx2* (**E**,**F**:11-12 somites; **G**,**H**: E9.5), *Nkx2.1* (**I**,**J**: 11-12 somites; **K**,**L**: E9.5), *Delta1* (**M**,**N**: 13-14 somites) and *Hes5* (**O**,**P**: 15-16 somites). Embryo genotypes are indicated above. Main panels are profile views, except in C,G,H (frontal views) and D,K,L (ventral views of the forebrain). Insets show profile views of the same embryos (C,D,G,H,K,L), or additional embryos at the 14- to 15-somite stage (E,F,I,J) or E9.5 (M,N). di, diencephalon; hb, hindbrain; mb, midbrain; te, telencephalon.

detected in the forebrain of both wild-type and *Raldh2*$^{-/-}$ embryos at the 10-somite stage (data not shown), at the 14-somite stage when *Delta1* is highly expressed in the wild-type telencephalic neuroepithelium, its expression was markedly reduced in the corresponding region of *Raldh2*$^{-/-}$ embryos (Fig. 5M,N). Eventually, *Delta1* expression was seen at E9.5 in the *Raldh2*$^{-/-}$ rudimentary forebrain neuroepithelium (Fig. 5M,N, insets). Similarly, expression of *Hes5* was defective in the E8.5 *Raldh2*$^{-/-}$ forebrain, although it was present in midbrain and hindbrain cells (Fig. 5O,P). At E9.5, *Hes5* expression was seen in the mutant forebrain neuroepithelium, albeit at lower levels than in wild type (data not shown). Thus, RA deficiency may affect the progression of neuronal differentiation in the embryonic forebrain by controlling genes of the lateral inhibition pathway.

Raldh2 activity is required for patterning of the optic vesicles and diencephalon

We also investigated the molecular alterations underlying abnormal development of the optic vesicles and Rathke's pouch in *Raldh2*$^{-/-}$ mutants. *Pax6* is a master gene for eye development (for a review, see Ashery-Padan and Gruss, 2001) that is also involved in diencephalon and telencephalon patterning (Stoykova et al., 1996; Stoykova et al., 2000). Its induction was not affected by RA deficiency, as normal PAX6 protein levels were detected in the forebrain neuroepithelium of six- to eight-somite stage *Raldh2*$^{-/-}$ embryos (data not shown). From the 10-somite stage in wild-type embryos, PAX6 levels are upregulated in the dorsal optic vesicle neuroepithelium, whereas the dorsal diencephalon and telencephalon display intermediate protein levels (Fig. 6A,C,D). PAX6 was not upregulated in the optic vesicle of *Raldh2*$^{-/-}$ embryos to the same extent as in wild-type embryos (Fig. 6B,D). Thus, its levels in the mutant optic vesicle were comparable with those seen in the dorsal diencephalon and telencephalon (Fig. 6D,D′).

Six3, a homologue of the *Drosophila sine oculis* gene, has been shown to promote anterior fate within the prospective forebrain (Lagutin et al., 2003). *Six3* expression in the ventral forebrain and optic vesicles was comparable in *Raldh2*$^{-/-}$ and wild-type embryos until the 10-somite stage (data not shown), but became abnormally low in the optic vesicles of mutants by the 12- to 14-somite stages (Fig. 6E,F). Expression of its homologue *Six6* (*Optx2*) was similarly reduced in the *Raldh2*$^{-/-}$ optic vesicles (Fig. 6E,F, insets). Altogether, these results indicate that RA signaling is required for the proper upregulation of the *Pax6* and *Six* genes within the optic vesicle. This regulation is gene specific as *Pax2*, which also controls eye development (Nornes et al., 1990), was expressed at normal levels in the optic vesicles of *Raldh2*$^{-/-}$ mutants, even at E9.5 (Fig. 6G,H).

To assess hypothalamic and infundibulum patterning, we analyzed *Hesx1* expression. This gene is normally expressed in the rostral neural folds, which resolve to the hypothalamus (Hermesz et al., 1996) (Fig. 6G), and its disruption leads to septo-optic dysplasia (Dattani et al., 1998). *Hesx1* expression was abnormally low in *Raldh2*$^{-/-}$ embryos from the 12-somite stage, especially within the infundibulum (Fig. 6I,J). Interestingly, expression of *Six3* and *Six6*, which are involved in neurohypophysis and hypothalamus development (Lagutin et al., 2003), was absent in the infundibulum of mutants (Fig. 6E,F, brackets; data not shown). Expression of *Bmp4*, another determinant of pituitary formation (Takuma et al., 1998; Ericson et al., 1998), was maintained in the infundibulum of *Raldh2*$^{-/-}$ embryos (Fig. 6K,L). These data suggest that molecular alterations intrinsic to the hypothalamus and infundibulum would affect development of Rathke's pouch in *Raldh2*$^{-/-}$ mutants.

RA deficiency affects FGF signaling in the craniofacial region

FGF8 is one of the key signals produced by the ANR, a secondary forebrain 'organizer' that controls both the outgrowth and specification of telencephalic territories (Crossley et al., 2001; Ohkubo et al., 2002; Storm et al., 2003; Echevarria et al., 2003). *Fgf8* was expressed at comparable levels in the ANR of wild-type and *Raldh2*$^{-/-}$ embryos at the 10- to 14-somite stages (Fig. 7A,B). Its expression was maintained in the ANR of mutants at E9.5, although section analysis showed weaker labeling than in its wild-type counterpart (Fig. 7C,D, compare insets, brackets). However, *Fgf8* induction was deficient in the facial surface ectoderm: only few *Fgf8*-positive cells were detected outside of the ANR in *Raldh2*$^{-/-}$ embryos (Fig. 7C,D).

As an indicator of effective intracellular FGF signaling, we assessed the levels of phosphorylated ERK1 and 2 (p-ERK1/2) (Corson et al., 2003) by whole-mount immunostaining. Between the 8 and 12 somite stages, p-ERK1/2 levels were comparable between wild-type and *Raldh2*$^{-/-}$ embryos. Slight reduction in immunostaining first appeared at the 14-somite stage (data not shown), whereas p-ERK1/2 levels were clearly decreased along the

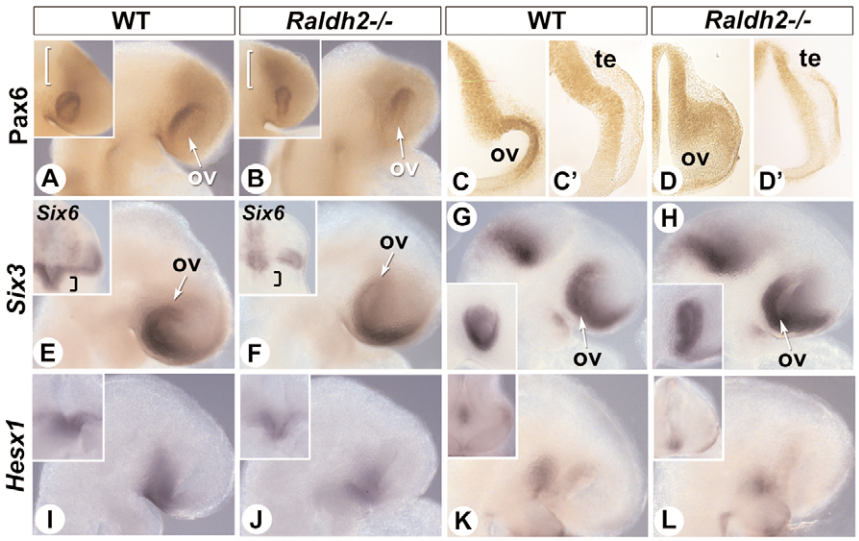

Fig. 6. Molecular analysis of the optic vesicle and infundibulum in *Raldh2*$^{-/-}$ embryos. (**A**,**B**) Whole-mount immunodetection of PAX6 protein in 10- to 11-somite stage (main panels) and 20- to 22-somite stage (insets) embryos. Profile views. Brackets indicate PAX6 expression in the dorsal telencephalon and diencephalon. (**C**-**D**′) PAX6 immunohistochemistry on frontal sections through the optic vesicle (C,D) and telencephalon (C′,D′) of wild-type and *Raldh2*$^{-/-}$ embryos (13-14 somites). (**E**-**L**) Whole-mount in situ hybridization of *Six3* (E,F), *Pax2* (G,H), *Hesx1* (I,J) and *Bmp4* (K,L) in 12- to 14-somite stage embryos. Genotypes are indicated above. Profile views. Insets in E,F show frontal views of *Six6*-hybridized embryos (brackets indicate infundibulum). Other insets show details of the optic vesicle of E9.5 embryos (G,H) or ventral views of the same embryos (I-L). ov, optic vesicle; te, telencephalon.

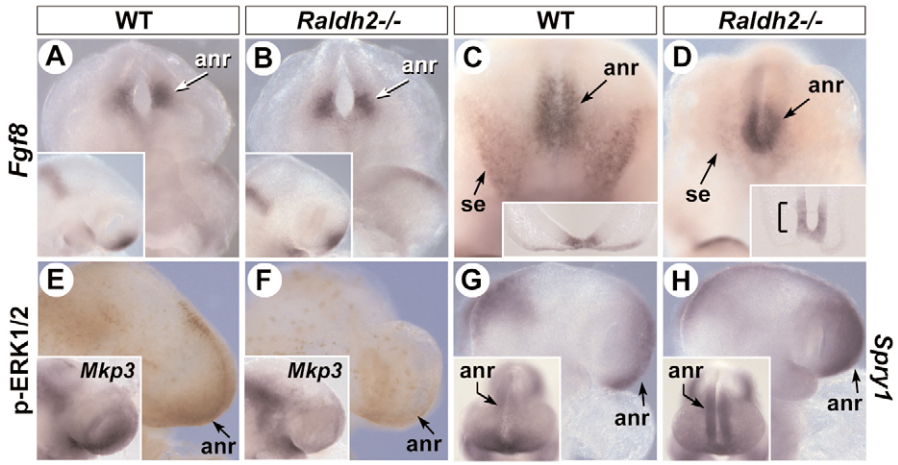

Fig. 7. Molecular analysis of Fgf gene expression and signaling in *Raldh2*$^{-/-}$ embryos. (**A**-**D**) Whole-mount *Fgf8* in situ hybridization on 13- to 14-somite stage (A,B) and E9.5 (C,D) embryos. Main panels: frontal views of the ANR. Insets show profile views (A,B) or transverse sections (C,D) of the same embryos. (**E**,**F**) Whole-mount p-ERK1/2 immunodetection (main panels, E9.5) and *Mkp3* in situ hybridization (insets, 12- to 14-somite stage). Profile views. (**G**,**H**) Whole-mount *Spry1* in situ hybridization on 12- to 14-somite stage embryos (main panels, profile views; insets, frontal views). Genotypes are indicated above. anr, anterior neural ridge; se, surface ectoderm.

ANR and anterior head ectoderm of E9.5 mutants (Fig. 7E,F). Expression of *Mkp3*, a negative feedback modulator of FGF signaling whose induction is FGF dependent (Kawakami et al., 2003; Echevarria et al., 2005), was almost undetectable in the anterior head mesenchyme of *Raldh2*$^{-/-}$ embryos (Fig. 7E,F, insets). Expression of sprouty 1 (*Spry1*), another FGF-dependent intracellular inhibitor (Hanafusa et al., 2002; Storm et al., 2003), was similarly decreased in rostral head tissues of mutant embryos, except in the ANR, where its expression was higher than in wild-type embryos from the 12-somite stage onwards (Fig. 7G,H).

RA deficiency affects Sonic hedgehog signaling in the forebrain

As the specification of ventral forebrain structures, which are affected by RA deficiency (see Figs 4, 5), relies on SHH activity (Ericson et al., 1995; Chiang et al., 1996; Gunhaga et al., 2000), we assessed whether SHH signaling may be altered in *Raldh2*$^{-/-}$ embryos. *Shh* is initially expressed in the prechordal plate underlying the neural tube (Fig. 8A). This activity controls the specification of ventral telencephalic structures (Ericson et al., 1995; Gunhaga et al., 2000) and downregulation of *Shh* expression has been observed in the prechordal plate of RA-deficient quail embryos (Halilagic et al., 2003). However, *Shh* expression was not altered in the prechordal plate of *Raldh2*$^{-/-}$ embryos at presomitic stages (Fig. 8B). Later on, *Shh* is induced along the neural tube floor plate up to the diencephalic level (Ericson et al., 1995) (Fig. 8C). No alteration of *Shh* expression was detected in the *Raldh2*$^{-/-}$ forebrain until the 16-somite stage (data not shown). From this stage, an abnormal downregulation was selectively observed in the rostral diencephalon, anterior to the presumptive zona limitans intrathalamica (ZLI) (Fig. 8D, bracket). In wild-type embryos, *Shh* expression is downregulated by E9.5 in the infundibulum region (Shimamura et al., 1995) (inset in Fig. 8C). In *Raldh2*$^{-/-}$ embryos, its expression was maintained within this region (Fig. 8D, inset), correlating with a rostral expansion of *Shh* expression along the ventralmost floor plate cells in younger mutants (Fig. 8D, arrow).

To assess the efficiency of SHH signaling, we analyzed downstream targets of this pathway. Expression of the SHH receptor patched depends on SHH activity (Goodrich et al., 1996; Marigo and Tabin, 1996). Patched (*Ptch1*) is expressed at high levels in the diencephalic neuroepithelium and surrounding mesenchyme of 12- to 14-somite stage wild-type embryos (Fig. 8E). *Ptch1* expression was abnormally low in the diencephalic neuroepithelium, and undetectable in the mesenchyme, of *Raldh2*$^{-/-}$ littermates (Fig. 8F; data not shown). At E9.5, *Ptch1* was no longer detected in the mutant diencephalon, except in its rostroventral area close to the optic vesicles (data not shown). Another direct target of SHH, *Gli1* (Lee et al., 1997), is normally expressed in the ventral diencephalic

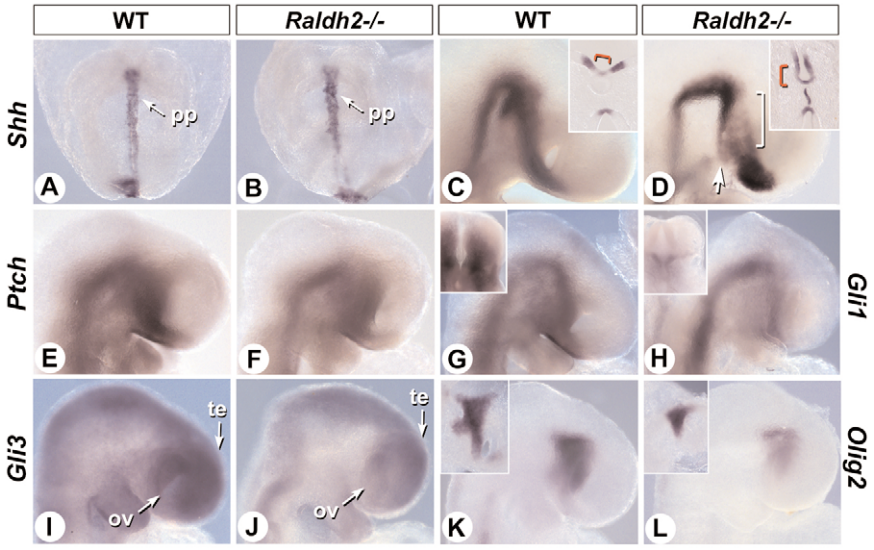

Fig. 8. Molecular analysis of SHH signaling in *Raldh2*$^{-/-}$ embryos. Whole-mount in situ hybridization with *Shh* (**A**-**D**), *Ptch1* (**E**,**F**), *Gli1* (**G**,**H**), *Gli3* (**I**,**J**) and *Olig2* (**K**,**L**) probes. Embryos are at E7.75 (A,B), E9.5 (C,D) and 12-15 somites (E-L). Profile views, except in A,B (ventral views). Insets show transverse sections of the infundibulum (red brackets, C,D), ventral views of the same embryos (G,H) or details of the *Olig2*-positive region in older (E9.5) embryos (K,L). Genotypes are indicated above. ov, optic vesicle; pp, prechordal plate; te, telencephalon.

neuroepithelium and surrounding mesenchyme, adjacent to the *Shh* expression domain (Fig. 8G). From the 10-somite stage, *Gli1* expression was reduced in the diencephalon and abolished in the mesenchyme of mutant embryos (Fig. 8H). At E9.5, *Gli1* transcripts were barely detectable in the mutant diencephalon, except in its rostroventral area (Fig. 8G,H, insets).

GLI3 is a peculiar component of the SHH pathway, which primarily functions as a repressor. Among various murine Gli mutants, only *Gli3*$^{-/-}$ embryos exhibit patterning defects in the forebrain, including downregulation of Emx genes and *Pax6* (Theil et al., 1999; Tole et al., 2000). In 14-somite stage wild-type embryos, *Gli3* is expressed in the dorsal diencephalon, the dorsal optic vesicle neuroepithelium and the telencephalon (Fig. 8I). From the 10- to 12-somite stages, *Gli3* expression was reduced in mutants, especially in the optic vesicle (Fig. 8J). Expression was comparatively less affected along the rostral telencephalon.

SHH has been implicated in the specification of forebrain oligodendrocyte precursors (OLPs) through the regulation of the *Olig1/2* genes (Nery et al., 2001; Tekki-Kessaris et al., 2001). OLPs first appear in the embryonic mouse diencephalon by E9 (Timsit et al., 1995), and region-specific *Olig2* expression is observed 1 day earlier in the wild-type diencephalon (Fig. 8K). The *Olig2*-expressing domain was diminished in E8.5 *Raldh2*$^{-/-}$ embryos and expression was lacking along the ventral diencephalon (Fig. 8L). A smaller *Olig2* domain was also seen at E9.5 in mutants (Fig. 8K,L, insets). This result, along with the defective induction of other SHH downstream genes such as *Nkx2.1* (Pabst et al., 2000) (see Fig. 5), strengthens the idea that SHH signaling activity is deficient in the diencephalon of RA-deficient embryos.

DISCUSSION

A mammalian model of RA deficiency during early forebrain development

Many neuroregulatory roles for RA have been proposed, including induction of spinal cord neuronal differentiation, potentiation of neurite outgrowth and localized induction of motoneuron production (reviewed by McCaffery et al., 2003; Appel and Eisen, 2003; Diez del Corral and Storey, 2004). Owing to the sequential expression of the *Raldh2* and *Raldh3* enzymes (Wagner et al., 2000; Li et al., 2000; Smith et al., 2001), RA production and signaling emerge in specific regions of the forebrain neuroepithelium and adjacent tissues while these regions undergo a dramatic burst of growth and remodeling. Here, we show that *Raldh2* is responsible for early RA production within the mouse embryonic head between the eight- and 14- to 15-somite stages. During this time window, no activity of the RARE-*lacZ* reporter transgene is detected in *Raldh2*$^{-/-}$ embryos, despite a normal onset of *Raldh3* gene expression in the head surface ectoderm. RALDH3 activity is likely to account for the subsequent activation of the RA-reporter transgene in the facial mesenchyme and surface ectoderm of the mutant embryos. However, it is unable to significantly activate the reporter transgene within the forebrain and optic neuroepithelium, even at E9.5.

Raldh2$^{-/-}$ embryos exhibit defective morphogenesis of several forebrain derivatives, including the telencephalic vesicles, the optic vesicles (see Mic et al., 2004a) and the diencephalon. Their forebrain-derived neural crest cells massively migrate towards the preoptic region, leading to an excess of mesenchyme that may contribute to the phenotypic abnormalities, e.g. by interfering with optic vesicle morphogenesis and lens placode induction. Complex molecular alterations underlie these defects. Although the early induction of several regulators of forebrain development (e.g. *Foxg1* or *Pax6*) is unaltered, we show that RALDH2-mediated RA synthesis is required for the maintenance of their normal levels of expression. The earliest molecular alterations (e.g. *Nkx2.1*) precede the morphological defects and are found in the ventral diencephalon. Expression of specific neural determinants of the optic vesicle and hypothalamic/infundibulum region (e.g. *Pax6*, *Six3*, *Six6*) is also affected and may contribute, respectively, to the eye and pituitary defects in mutants.

RA deficiency affects FGF signaling in the forebrain

RA deficiency caused by *Raldh2* loss of function interferes with two major signaling pathways that regulate forebrain development: the SHH and FGF pathways. *Fgf8* induction proceeds normally in the ANR of *Raldh2*$^{-/-}$ embryos; at E9.5, its expression is only marginally decreased. However, *Fgf8* almost completely fails to be activated in the facial ectoderm of mutants. Reduced levels of phosphorylated ERK1/2, and of *Mkp3* and *Spry1* transcripts (which are normally induced in response to FGF) in the anterior head mesenchyme and surface ectoderm of mutants, collectively indicate impaired FGF signaling in these tissues. Unexpectedly, however, *Spry1* expression was found to be upregulated within the ANR of mutant embryos. We did not detect abnormal levels of other Fgf genes (*Fgf3*, *Fgf17* or *Fgf18*) in the craniofacial region of mutants, suggesting that this upregulation might be FGF independent. As *Spry1* encodes an intracellular inhibitor of FGF signaling (Hanafusa et al., 2002), its upregulation could participate to the defective FGF signaling within the ANR.

Decreased FGF signaling can explain several abnormalities in the RA-deficient embryos that have been similarly observed in other models where the FGF pathway was experimentally altered. Reduction of *Foxg1* and *Emx2* expression, as well as increased apoptosis, are seen following *Spry1* overexpression in mouse telencephalic explants (Storm et al., 2003). Inhibition of pERK signaling (Shinya et al., 2001) or *Fgf8* mutation (Shanmugalingam et al., 2000) in zebrafish lead to a reduction of the prospective medial ganglionic eminence, which is also seen in the *Raldh2*$^{-/-}$ embryos by *Nkx2.1* expression. Interestingly, correct expression of *Fgf8* in the chick ANR and head ectoderm has been shown to rely on facial NCCs (Creuzet et al., 2004). NCCs show an abnormal distribution in the frontonasal region of *Raldh2*$^{-/-}$ embryos and maintain high levels of *Ap2a* and *Sox10* expression, genes that are normally turned off when cells undergo differentiation (Kim et al., 2003; Mitchell et al., 1991). Impaired NCC-facial ectoderm interactions (and/or abnormal specification of NCCs) could therefore play a role in the defective *Fgf8* induction in the RA-deficient embryos.

Altered FGF signaling could also account for the cell proliferation defect observed in the forebrain neuroepithelium of mutants. FGF8 produced by the ANR induces *Foxg1* (Shimamura and Rubenstein, 1997), which then regulates regionalization and growth of the telencephalon by promoting the proliferation of neuroectodermal cells (Xuan et al., 1995; Martynoga et al., 2005). In *Xenopus*, *Foxg1* regulates expression of the cyclin-dependent kinase inhibitor p27 (Hardcastle and Papalopulu, 2000). In the *Raldh2*$^{-/-}$ mutants, downregulation of *Foxg1* is accompanied by regionally reduced expression of cyclin D2 and cyclin D3. D-cyclins are induced by mitogens and act as sensors of the extracellular environment that link mitogenic pathways to the core cell cycle machinery (reviewed by Sherr and Roberts, 2004). Their effect can be inhibited by the cyclin-dependent kinase inhibitors p21 and p27 (Sherr and Roberts, 1999). Increased *p21* expression, which was observed in the ventral forebrain neuroepithelium of E9.5 *Raldh2*$^{-/-}$ embryos, may further contribute to the cell proliferation defect.

RA is required for proper Sonic hedgehog signaling in head tissues

Analysis of the expression of two SHH direct target genes, *Gli1* and *Ptch1*, revealed decreased levels of SHH signaling in post-optic ectomesenchymal cells and diencephalic neuroepithelium of *Raldh2*$^{-/-}$ mutants, from the 10- to 12-somite stage onwards. This decrease is not linked to a downregulation of *Shh* itself, whose expression is not affected prior to the 16-somite stage in mutants. Altered SHH signaling is likely to be responsible for the early patterning defects observed in the *Raldh2*$^{-/-}$ ventral diencephalon. Studies in various models have demonstrated that ventral genes, such as *NKx2.1*, are downregulated or not induced when SHH signaling is impaired (Ericson et al., 1995; Gunhaga et al., 2000; Rallu et al., 2002b) and that pituitary development requires SHH signaling (Treier et al., 2001; Sbrogna et al., 2003). Accordingly, we find that key genes involved in infundibulum specification (such as *Six3*, *Six6* or *Hesx1*) are affected in the *Raldh2*$^{-/-}$ mutants. Whether our observations reflect a possible role of RA in regulating the processing of SHH to an active form or its transport (Okada et al., 2004), or the convergence of RA and SHH pathways for proper regulation of common target genes (Tsukui et al., 1999; Novitch et al., 2003; Schafer et al., 2005), remains to be clarified.

Abnormal SHH signaling might in turn affect the FGF pathway in the RA-deficient embryos. Several studies have shown that both in the forebrain and the limb bud a decrease in SHH signaling leads to a downregulation of Fgf gene expression (Sun et al., 2000; Kraus et al., 2001; Ohkubo et al., 2002). Thus, RA activity in the forebrain, as postulated for the limb (Helms et al., 1994; Schneider et al., 2001; Niederreither et al., 2002b; Mic et al., 2004b), would be required for the establishment of a functional FGF-SHH signaling loop. Schneider et al. (Schneider et al., 2001) have inhibited RAR/RXR signaling in the chick embryonic head, and have correlated the resulting forebrain and facial deficiencies to a loss of *Fgf8* and *Shh* expression. Our model of endogenous RA deficiency refines the relationship between these pathways, by showing that: (1) response to the SHH signal is affected before any detectable change in *Shh* expression; (2) *Fgf8* expression in the head ectoderm (rather than the ANR) is critically RA dependent; and (3) abnormal levels of *Spry1* might participate to the decreased FGF signaling in the ANR.

A model for RA action in the embryonic forebrain

The brain develops from multipotent, self-renewing stem cells that are defined by their ability, in vitro, to generate floating aggregates (neurospheres) capable of differentiating into neurons, astrocytes and oligodendrocytes (Reynolds and Weiss, 1992; Gritti et al., 1996). Among adult forebrain precursors there are stem-like cells that can be cultured in the presence of mitogens such as FGFs (Gritti et al., 1996; Johe et al., 1996). Embryonic dorsal neurospheres acquire *Olig2* expression (and oligodendrocyte identity) only after exposure to FGF, which promotes the ventralization of the stem cell population (Gabay et al., 2003). The mouse model of RA deficiency described herein offers insight into how RA regulates neural stem cell proliferation in a temporally regulated manner. A localized burst of ventrally enriched RA production occurs in the mouse forebrain at the 8- to 10-somite stages. We hypothesize this serves to 'prime' the ventralization of forebrain neural stem cell populations. In the absence of RA several events occur: (1) reduction in ventral forebrain gene expression; (2) impaired response to the SHH signal; and (3) at a later stage, reduced FGF signaling. The initial patterning alterations affect ventral neuronal determinants (such as *Nkx2.1*), as well as the oligodendrocyte determinant *Olig2*. Several hours later (after the 12- to 14-somite stages), RA acts in a broader manner, affecting both dorsal and ventral cell populations, as evidenced by the defective telencephalic vesicle outgrowth and overall thinning of the forebrain neuroepithelium in the *Raldh2*$^{-/-}$ embryos. Throughout these stages, a reduction in the expansion of neuronal progenitors, accompanied by cell survival changes, could account for the abnormal forebrain phenotype. The challenge will be to understand how crosstalk between RA, FGF and SHH signaling lead to their sequential actions in regulating stem cell cycle exit and induction of molecular determinants of patterning and/or cell-type specification.

We thank P. Chambon for constant support; F. Gofflot and I. Le Roux for critical comments; V. Fraulob and B. Schuhbaur for technical assistance; J. Rossant for the *RARE-hsp68-lacZ* mice; P. McCaffery for the RALDH2 antibody; and D. Anderson (*Olig2*), S. L. Ang (*FoxG1*), B. De Crombrugghe (*Sox9*), P. Gruss (*Pax2, Six3-6*), B. Hogan (*Bmp4*), C. C. Hui (*Gli1-3*), G. Martin (*Fgf8, Spry1*), A. McMahon (*Shh*), P. Minoo (*NKx2.1*), P. Mitchell (*AP2α*), C. Sherr (*Cyclins*) and A. Simeone (*Emx2*) for template plasmids. This work was supported by grants from the American Heart Association (0330265N) and the National Institute of Health (R01 HL070733) (to K.N.); and by funds from the CNRS, INSERM, Hôpitaux Universitaires de Strasbourg, Ministère Français de la Recherche (ACI 03-2-490), Institut Universitaire de France and European Union (EVI-GENORET: LSHG-CT-2005-512036) (to P.D.).

References

Appel, B. and Eisen, J. S. (2003). Retinoids run rampant: multiple roles during spinal cord and motor neuron development. *Neuron* **40**, 461-464.
Ashery-Padan, R. and Gruss, P. (2001). Pax6 lights-up the way for eye development. *Curr. Opin. Cell Biol.* **13**, 706-714.
Berggren, K., McCaffery, P., Drager, U. and Forehand, C. J. (1999). Differential distribution of retinoic acid synthesis in the chicken embryo as determined by immunolocalization of the retinoic acid synthetic enzyme, RALDH-2. *Dev. Biol.* **210**, 288-304.
Bettenhausen, B., Hrabe de Angelis, M., Simon, D., Guenet, J. L. and Gossler, A. (1995). Transient and restricted expression during mouse embryogenesis of Dll1, a murine gene closely related to Drosophila Delta. *Development* **121**, 2407-2418.
Blentic, A., Gale, E. and Maden, M. (2003). Retinoic acid signalling centres in the avian embryo identified by sites of expression of synthesising and catabolising enzymes. *Dev. Dyn.* **227**, 114-127.
Chambon, P. (1996). A decade of molecular biology of retinoic acid receptors. *FASEB J.* **10**, 940-954.
Chiang, C., Litingtung, Y., Lee, E., Young, K. E., Corden, J. L., Westphal, H. and Beachy, P. A. (1996). Cyclopia and defective axial patterning in mice lacking Sonic hedgehog gene function. *Nature* **383**, 407-413.
Chotteau-Lelièvre, A., Dollé, P. and Gofflot, F. (2005). Expression analysis of murine genes using in situ hybridization with radioactive and non-radioactively labeled probes. In *Methods in Molecular Biology: In Situ Hybridization Protocols*, 3rd edn (ed. I. A. Darby and T. D. Hewitson). Totowa (NJ): Humana Press.
Chow, R. L. and Lang, R. A. (2001). Early eye development in vertebrates. *Annu. Rev. Cell Dev. Biol.* **17**, 255-296.
Corson, L. B., Yamanaka, Y., Lai, K. M. and Rossant, J. (2003). Spatial and temporal patterns of ERK signaling during mouse embryogenesis. *Development* **130**, 4527-4537.
Creuzet, S., Schuler, B., Couly, G. and Le Douarin, N. M. (2004). Reciprocal relationships between *Fgf8* and neural crest cells in facial and forebrain development. *Proc. Natl. Acad. Sci. USA* **101**, 4843-4847.
Crossley, P. H., Martinez, S., Ohkubo, Y. and Rubenstein, J. L. (2001). Coordinate expression of Fgf8, Otx2, Bmp4, and Shh in the rostral prosencephalon during development of the telencephalic and optic vesicles. *Neuroscience* **108**, 183-206.
Dattani, M. T., Martinez-Barbera, J. P., Thomas, P. Q., Brickman, J. M., Gupta, R., Martensson, I. L., Toresson, H., Fox, M., Wales, J. K., Hindmarsh, P. C. et al. (1998). Mutations in the homeobox gene HESX1/Hesx1 associated with septo-optic dysplasia in human and mouse. *Nat. Genet.* **19**, 125-133.
Diez del Corral, R. and Storey, K. G. (2004). Opposing FGF and retinoid pathways: a signalling switch that controls differentiation and patterning onset in the extending vertebrate body axis. *BioEssays* **26**, 857-869.
Duester, G. (2001). Genetic dissection of retinoid dehydrogenases. *Chem. Biol. Interact.* **30**, 469-480.
Dupé, V., Matt, N., Garnier, J. M., Chambon, P., Mark, M. and Ghyselinck, N. B. (2003). A newborn lethal defect due to inactivation of retinaldehyde dehydrogenase type 3 is prevented by maternal retinoic acid treatment. *Proc. Natl. Acad. Sci. USA* **100**, 14036-14041.
Echevarria, D., Vieira, C., Gimeno, L. and Martinez, S. (2003). Neuroepithelial secondary organizers and cell fate specification in the developing brain. *Brain Res. Brain Res. Rev.* **43**, 179-191.
Echevarria, D., Martinez, S., Marques, S., Lucas-Teixeira, V. and Belo, J. A.

(2005). Mkp3 is a negative feedback modulator of Fgf8 signaling in the mammalian isthmic organizer. *Dev. Biol.* **277**, 114-128.
Ericson, J., Muhr, J., Placzek, M., Lints, T., Jessell, T. M. and Edlund, T. (1995). Sonic hedgehog induces the differentiation of ventral forebrain neurons: a common signal for ventral patterning within the neural tube. *Cell* **81**, 747-756.
Ericson, J., Norlin, S., Jessell, T. M. and Edlund, T. (1998). Integrated FGF and BMP signaling controls the progression of progenitor cell differentiation and the emergence of pattern in the embryonic anterior pituitary. *Development* **125**, 1005-1015.
Gabay, L., Lowell, S., Rubin, L. L. and Anderson, D. J. (2003). Deregulation of dorsoventral patterning by FGF confers trilineage differentiation capacity on CNS stem cells in vitro. *Neuron* **40**, 485-499.
Gong, Q. and Shipley, M. T. (1995). Evidence that pioneer olfactory axons regulate telencephalon cell cycle kinetics to induce the formation of the olfactory bulb. *Neuron* **14**, 91-101.
Goodrich, L. V., Johnson, R. L., Milenkovic, L., McMahon, J. A. and Scott, M. P. (1996). Conservation of the hedgehog/patched signaling pathway from flies to mice: induction of a mouse patched gene by Hedgehog. *Genes Dev.* **10**, 301-312.
Graham, A. and Begbie, J. (2000). Neurogenic placodes: a common front. *Trends Neurosci.* **23**, 313-316.
Gritti, A., Parati, E. A., Cova, L., Frolichsthal, P., Galli, R., Wanke, E., Faravelli, L., Morassutti, D. J., Roisen, F., Nickel, D. D. et al. (1996). Multipotential stem cells from the adult mouse brain proliferate and self-renew in response to basic fibroblast growth factor. *J. Neurosci.* **16**, 1091-1100.
Gunhaga, L., Jessell, T. M. and Edlund, T. (2000). Sonic hedgehog signaling at gastrula stages specifies ventral telencephalic cells in the chick embryo. *Development* **127**, 3283-3293.
Halilagic, A., Zile, M. H. and Studer, M. (2003). A novel role for retinoids in patterning the avian forebrain during presomite stages. *Development* **130**, 2039-2050.
Hanafusa, H., Torii, S., Yasunaga, T. and Nishida, E. (2002). Sprouty1 and Sprouty2 provide a control mechanism for the Ras/MAPK signalling pathway. *Nat. Cell Biol.* **4**, 850-858.
Hardcastle, Z. and Papalopulu, N. (2000). Distinct effects of XBF-1 in regulating the cell cycle inhibitor p27(XIC1) and imparting a neural fate. *Development* **127**, 1303-1314.
Hatakeyama, J., Bessho, Y., Katoh, K., Ookawara, S., Fujioka, M., Guillemot, F. and Kageyama, R. (2004). Hes genes regulate size, shape and histogenesis of the nervous system by control of the timing of neural stem cell differentiation. *Development* **131**, 5539-5550.
Helms, J., Thaller, C. and Eichele, G. (1994). Relationship between retinoic acid and sonic hedgehog, two polarizing signals in the chick wing bud. *Development* **120**, 3267-3274.
Hermesz, E., Mackem, S. and Mahon, K. A. (1996). Rpx: a novel anterior-restricted homeobox gene progressively activated in the prechordal plate, anterior neural plate and Rathke's pouch of the mouse embryo. *Development* **122**, 41-52.
Johe, K. K., Hazel, T. G., Muller, T., Dugich-Djordjevic, M. M. and McKay, R. D. (1996). Single factors direct the differentiation of stem cells from the fetal and adult central nervous system. *Genes Dev.* **10**, 3129-3140.
Kawakami, Y., Rodriguez-Leon, J., Koth, C. M., Buscher, D., Itoh, T., Raya, A., Ng, J. K., Esteban, C. R., Takahashi, S., Henrique, D. et al. (2003). MKP3 mediates the cellular response to FGF8 signalling in the vertebrate limb. *Nat. Cell Biol.* **5**, 513-519.
Kim, J., Lo, L., Dormand, E. and Anderson, D. J. (2003). SOX10 maintains multipotency and inhibits neuronal differentiation of neural crest stem cells. *Neuron* **38**, 17-31.
Kobayashi, D., Kobayashi, M., Matsumoto, K., Ogura, T., Nakafuku, M. and Shimamura, K. (2002). Early subdivisions in the neural plate define distinct competence for inductive signals. *Development* **129**, 83-93.
Kraus, P., Fraidenraich, D. and Loomis, C. A. (2001). Some distal limb structures develop in mice lacking Sonic hedgehog signaling. *Mech. Dev.* **100**, 45-58.
Lagutin, O. V., Zhu, C. C., Kobayashi, D., Topczewski, J., Shimamura, K., Puelles, L., Russell, H. R., McKinnon, P. J., Solnica-Krezel, L. and Oliver, G. (2003). Six3 repression of Wnt signaling in the anterior neuroectoderm is essential for vertebrate forebrain development. *Genes Dev.* **17**, 368-379.
Lee, J., Platt, K. A., Censullo, P. and Ruiz i Altaba, A. (1997). Gli1 is a target of Sonic hedgehog that induces ventral neural tube development. *Development* **124**, 2537-2552.
Li, H., Wagner, E., McCaffery, P., Smith, D., Andreadis, A. and Dräger, U. C. (2000). A retinoic acid synthesizing enzyme in ventral retina and telencephalon of the embryonic mouse. *Mech. Dev.* **95**, 283-289.
Lohnes, D., Mark, M., Mendelsohn, C., Dollé, P., Dierich, A., Gorry, P., Gansmuller, A. and Chambon, P. (1994). Function of the retinoic acid receptors (RARs) during development (I). Craniofacial and skeletal abnormalities in RAR double mutants. *Development* **120**, 2723-2748.
Marigo, V. and Tabin, C. J. (1996). Regulation of patched by sonic hedgehog in the developing neural tube. *Proc. Natl. Acad. Sci. USA* **93**, 9346-9351.
Marklund, M., Sjodal, M., Beehler, B. C., Jessell, T. M., Edlund, T. and Gunhaga, L. (2004). Retinoic acid signalling specifies intermediate character in the developing telencephalon. *Development* **131**, 4323-4332.
Martynoga, B., Morrison, H., Price, D. J. and Mason, J. O. (2005). Foxg1 is required for specification of ventral telencephalon and region-specific regulation of dorsal telencephalic precursor proliferation and apoptosis. *Dev. Biol.* **283**, 113-127.
McCaffery, P. J., Adams, J., Maden, M. and Rosa-Molinar, E. (2003). Too much of a good thing: retinoic acid as an endogenous regulator of neural differentiation and exogenous teratogen. *Eur. J. Neurosci.* **18**, 457-472.
Mic, F. A., Molotkov, A., Molotkova, N. and Duester, G. (2004a). Raldh2 expression in optic vesicle generates a retinoic acid signal needed for invagination of retina during optic cup formation. *Dev. Dyn.* **231**, 270-277.
Mic, F. A., Sirbu, I. O. and Duester, G. (2004b). Retinoic acid synthesis controlled by Raldh2 is required early for limb bud initiation and then later as a proximodistal signal during apical ectodermal ridge formation. *J. Biol. Chem.* **279**, 26698-26706.
Mitchell, P. J., Timmons, P. M., Hebert, J. M., Rigby, P. W. and Tjian, R. (2001). **T**ranscription factor AP-2 is expressed in neural crest cell lineages during mouse embryogenesis. *Genes Dev.* **91**, 105-119.
Mollard, R., Viville, S., Ward, S. J., Decimo, D., Chambon, P. and Dollé, P. (2000). Tissue-specific expression of retinoic acid receptor isoform transcripts in the mouse embryo. *Mech. Dev.* **94**, 223-232.
Mori-Akiyama, Y., Akiyama, H., Rowitch, D. H. and de Crombrugghe, B. (2003). Sox9 is required for determination of the chondrogenic cell lineage in the cranial neural crest. *Proc. Natl. Acad. Sci. USA* **100**, 9360-9365.
Nery, S., Wichterle, H. and Fishell, G. (2001). Sonic hedgehog contributes to oligodendrocyte specification in the mammalian forebrain. *Development* **128**, 527-540.
Niederreither, K., Subbarayan, V., Dollé, P. and Chambon, P. (1999). Embryonic retinoic acid synthesis is essential for early mouse post-implantation development. *Nat. Genet.* **21**, 444-448.
Niederreither, K., Vermot, J., Messaddeq, N., Schuhbaur, B., Chambon, P. and Dollé, P. (2001). Embryonic retinoic acid synthesis is essential for heart morphogenesis in the mouse. *Development* **128**, 1019-1031.
Niederreither, K., Vermot, J., Fraulob, V., Chambon, P. and Dollé, P. (2002a). Retinaldehyde dehydrogenase 2 (RALDH2)- independent patterns of retinoic acid synthesis in the mouse embryo. *Proc. Natl. Acad. Sci. USA* **99**, 16111-16116.
Niederreither, K., Vermot, J., Schuhbaur, B., Chambon, P. and Dollé, P. (2002b). Embryonic retinoic acid synthesis is required for forelimb growth and anteroposterior patterning in the mouse. *Development* **129**, 3563-3574.
Nornes, H. O., Dressler, G. R., Knapik, E. W., Deutsch, U. and Gruss, P. (1990). Spatially and temporally restricted expression of Pax2 during murine neurogenesis. *Development* **109**, 797-809.
Novitch, B. G., Wichterle, H., Jessell, T. M. and Sockanathan, S. (2003). A requirement for retinoic acid-mediated transcriptional activation in ventral neural patterning and motor neuron specification. *Neuron* **40**, 81-95.
Ohkubo, Y., Chiang, C. and Rubenstein, J. L. (2002). Coordinate regulation and synergistic actions of BMP4, SHH and FGF8 in the rostral prosencephalon regulate morphogenesis of the telencephalic and optic vesicles. *Neuroscience* **111**, 1-17.
Okada, Y., Shimazaki, T., Sobue, G. and Okano, H. (2004). Retinoic-acid-concentration-dependent acquisition of neural cell identity during in vitro differentiation of mouse embryonic stem cells. *Dev. Biol.* **275**, 124-142.
Osumi-Yamashita, N., Ninomiya, Y., Doi, H. and Eto, K. (1994). The contribution of both forebrain and midbrain crest cells to the mesenchyme in the frontonasal mass of mouse embryos. *Dev. Biol.* **164**, 409-419.
Pabst, O., Herbrand, H., Takuma, N. and Arnold, H. H. (2000). NKX2 gene expression in neuroectoderm but not in mesendodermally derived structures depends on sonic hedgehog in mouse embryos. *Dev. Genes Evol.* **210**, 47-50.
Pera, E. M. and Kessel, M. (1997). Patterning of the chick forebrain anlage by the prechordal plate. *Development* **124**, 4153-4162.
Puelles, L. and Rubenstein, J. L. (2003). Forebrain gene expression domains and the evolving prosomeric model. *Trends Neurosci.* **26**, 469-476.
Rallu, M., Corbin, J. G. and Fishell, G. (2002a). Parsing the prosencephalon. *Nat. Rev. Neurosci.* **3**, 943-951.
Rallu, M., Machold, R., Gaiano, N., Corbin, J. G., McMahon, A. P. and Fishell, G. (2002b). Dorsoventral patterning is established in the telencephalon of mutants lacking both Gli3 and Hedgehog signaling. *Development* **129**, 4963-4974.
Reynolds, B. A. and Weiss, S. (1992). Generation of neurons and astrocytes from isolated cells of the adult mammalian central nervous system. *Science* **255**, 1707-1710.
Rossant, J., Zirngibl, R., Cado, D., Shago, M. and Giguère, V. (1991). Expression of a retinoic acid response element-hsplacZ transgene defines specific domains of transcriptional activity during mouse embryogenesis. *Genes Dev.* **5**, 1333-1344.
Ruberte, E., Dollé, P., Chambon, P. and Morriss-Kay, G. (1991). Retinoic acid receptors and cellular retinoid binding proteins. II. Their differential pattern of transcription during early morphogenesis in mouse embryos. *Development* **111**, 45-60.

Sbrogna, J. L., Barresi, M. J. and Karlstrom, R. O. (2003). Multiple roles for Hedgehog signaling in zebrafish pituitary development. *Dev. Biol.* **254**, 19-35.
Scardigli, R., Baumer, N., Gruss, P., Guillemot, F. and Le Roux, I. (2003). Direct and concentration-dependent regulation of the proneural gene Neurogenin2 by Pax6. *Development* **130**, 3269-3281.
Schafer, M., Kinzel, D., Neuner, C., Schartl, M., Volff, J. N. and Winkler, C. (2005). Hedgehog and retinoid signalling confines nkx2.2b expression to the lateral floor plate of the zebrafish trunk. *Mech. Dev.* **122**, 43-56.
Schneider, R. A., Hu, D., Rubenstein, J. L., Maden, M. and Helms, J. A. (2001). Local retinoid signaling coordinates forebrain and facial morphogenesis by maintaining FGF8 and SHH. *Development* **128**, 2755-2767.
Serbedzija, G. N., Bronner-Fraser, M. and Fraser, S. E. (1992). Vital dye analysis of cranial neural crest cell migration in the mouse embryo. *Development* **116**, 297-307.
Shanmugalingam, S., Houart, C., Picker, A., Reifers, F., Macdonald, R., Barth, A., Griffin, K., Brand, M. and Wilson, S. W. (2000). Ace/Fgf8 is required for forebrain commissure formation and patterning of the telencephalon. *Development* **127**, 2549-2561.
Sherr, C. J. and Roberts, J. M. (1999). CDK inhibitors: positive and negative regulators of G1-phase progression. *Genes Dev.* **13**, 1501-1512.
Sherr, C. J. and Roberts, J. M. (2004). Living with or without cyclins and cyclin-dependent kinases. *Genes Dev.* **18**, 2699-2711.
Shimamura, K. and Rubenstein, J. L. (1997). Inductive interactions direct early regionalization of the mouse forebrain. *Development* **124**, 2709-2718.
Shimamura, K., Hartigan, D. J., Martinez, S., Puelles, L. and Rubenstein, J. L. (1995). Longitudinal organization of the anterior neural plate and neural tube. *Development* **121**, 3923-3933.
Shimamura, K., Martinez, S., Puelles, L. and Rubenstein, J. L. (1997). Patterns of gene expression in the neural plate and neural tube subdivide the embryonic forebrain into transverse and longitudinal domains. *Dev. Neurosci.* **19**, 88-96.
Shinya, M., Koshida, S., Sawada, A., Kuroiwa, A. and Takeda, H. (2001). Fgf signalling through MAPK cascade is required for development of the subpallial telencephalon in zebrafish embryos. *Development* **128**, 4153-4164.
Simeone, A., Gulisano, M., Acampora, D., Stornaiuolo, A., Rambaldi, M. and Boncinelli, E. (1992). Two vertebrate homeobox genes related to the Drosophila empty spiracles gene are expressed in the embryonic cerebral cortex. *EMBO J.* **11**, 2541-2550.
Smith, D., Wagner, E., Koul, O., McCaffery, P. and Dräger, U. C. (2001). Retinoic acid synthesis for the developing telencephalon. *Cereb. Cortex* **11**, 894-905.
Stoilov, I., Jansson, I., Sarfarazi, M. and Schenkman, J. B. (2001). Roles of cytochrome p450 in development. *Drug Metabol. Drug Interact.* **18**, 33-55.
Storm, E. E., Rubenstein, J. L. and Martin, G. R. (2003). Dosage of Fgf8 determines whether cell survival is positively or negatively regulated in the developing forebrain. *Proc. Natl. Acad. Sci. USA* **100**, 1757-1762.
Stoykova, A., Fritsch, R., Walther, C. and Gruss, P. (1996). Forebrain patterning defects in Small eye mutant mice. *Development* **122**, 3453-3465.
Stoykova, A., Treichel, D., Hallonet, M. and Gruss, P. (2000). Pax6 modulates the dorsoventral patterning of the mammalian telencephalon. *J. Neurosci.* **20**, 8042-8050.
Sun, X., Lewandoski, M., Meyers, E. N., Liu, Y. H., Maxson, R. E., Jr and Martin, G. R. (2000). Conditional inactivation of Fgf4 reveals complexity of signalling during limb bud development. *Nat. Genet.* **25**, 83-86.
Takuma, N., Sheng, H. Z., Furuta, Y., Ward, J. M., Sharma, K., Hogan, B. L., Pfaff, S. L., Westphal, H., Kimura, S. and Mahon, K. A. (1998). Formation of Rathke's pouch requires dual induction from the diencephalon. *Development* **125**, 4835-4840.
Tekki-Kessaris, N., Woodruff, R., Hall, A. C., Gaffield, W., Kimura, S., Stiles, C. D., Rowitch, D. H. and Richardson, W. D. (2001). Hedgehog-dependent oligodendrocyte lineage specification in the telencephalon. *Development* **128**, 2545-2554.
Theil, T., Alvarez-Bolado, G., Walter, A. and Ruther, U. (1999). Gli3 is required for Emx gene expression during dorsal telencephalon development. *Development* **126**, 3561-3571.
Timsit, S., Martinez, S., Allinquant, B., Peyron, F., Puelles, L. and Zalc, B. (1995). Oligodendrocytes originate in a restricted zone of the embryonic ventral neural tube defined by DM-20 mRNA expression. *J. Neurosci.* **15**, 1012-1024.
Tole, S., Ragsdale, C. W. and Grove, E. A. (2000). Dorsoventral patterning of the telencephalon is disrupted in the mouse mutant extra-toes(J). *Dev. Biol.* **217**, 254-265.
Treier, M., O'Connell, S., Gleiberman, A., Price, J., Szeto, D. P., Burgess, R., Chuang, P. T., McMahon, A. P. and Rosenfeld, M. G. (2001). Hedgehog signaling is required for pituitary gland development. *Development* **128**, 377-386.
Tsukui, T., Capdevila, J., Tamura, K., Ruiz-Lozano, P., Rodriguez-Esteban, C., Yonei-Tamura, S., Magallon, J., Chandraratna, R. A., Chien, K., Blumberg, B. et al. (1999). Multiple left-right asymmetry defects in Shh(–/–) mutant mice unveil a convergence of the shh and retinoic acid pathways in the control. of Lefty-1. *Proc. Natl. Acad. Sci. USA* **96**, 11376-11381.
Wagner, E., McCaffery, P. and Dräger, U. C. (2000). Retinoic acid in the formation of the dorsoventral retina and its central projections. *Dev. Biol.* **222**, 460-470.
Wianny, F., Real, F. X., Mummery, C. L., Van Rooijen, M., Lahti, J., Samarut, J. and Savatier, P. (1998). G1-phase regulators, cyclin D1, cyclin D2, and cyclin D3: up-regulation at gastrulation and dynamic expression during neurulation. *Dev. Dyn.* **212**, 49-62.
Wilson, S. W. and Houart, C. (2004). Early steps in the development of the forebrain. *Dev. Cell* **6**, 167-181.
Xuan, S., Baptista, C. A., Balas, G., Tao, W., Soares, V. C. and Lai, E. (1995). Winged helix transcription factor BF-1 is essential for the development of the cerebral hemispheres. *Neuron* **14**, 1141-1152.